Pergamon

0017-9310(95)00060-7

Role of micro-convection due to non-affine motion of particles in a mono-disperse suspension

SUNIL K. GUPTE and SURESH G. ADVANI†

Department of Mechanical Engineering, University of Delaware, Newark, DE 19711, U.S.A.

and

PABLO HUQ

College of Marine Studies, University of Delaware, Newark, DE 19711, U.S.A.

Abstract—Non-affine translation of suspended particles in a flowing suspension causes micro-convection of the fluid in the vicinity of the particle which affects the local transport mechanisms in the suspension. To investigate the importance of micro-convection on heat transport, a unit cell approach is adopted. A parametric study investigates the influence of particle fall velocity in a quiescent fluid and particle volume fraction on micro-convection in a sedimenting suspension. The thermal flux across the unit cell is shown to be a function of modified Péclet number that includes the influence of volume fraction for the range of volume fractions $(0 < \varepsilon < 0.3)$ and for $Pe \sim O(1)$. This is used to investigate the influence of hindered settling on transport processes such as heat transfer occurring in a sedimenting suspension.

1. INTRODUCTION

It is well-known that heat transfer rates in two-phase systems are generally higher than in single phase fluids under similar flow conditions. This enhancement may be attributed to many physical processes that occur in a two-phase flow, namely micro-convection around solid inclusions, phase changes and associated effects due to latent heat, additional turbulence because of the presence of inclusions, non-affine motion of suspended particles, thermal properties of suspended particles and, finally, velocity gradients near flow boundaries can have a significant affect on heat transfer rates and the mechanisms of heat transfer [1, 2]. A model to predict effective thermal conductivity of suspensions where there is relative motion between the suspended particles and the fluid was developed for a dilute suspension undergoing simple shear at low Péclet number [3].

Heat transfer occurring in fluid/solid mixtures is important from the viewpoint of industrial applications which range from processing of slurries and gaseous suspensions to manufacturing of polymer composite materials. This wide spectrum also includes very critical applications such as cooling of nuclear reactors using gas–ceramic mixtures, processing of food and spray drying of milk. In almost all chemical processing, one requires precise temperature control,

consequently, one requires detailed understanding of heat transfer mechanisms.

Whenever a suspended phase moves non-affinely during a flow process, mechanical dispersion gives rise to a heat transfer mechanism which is distinctly different from either pure conduction or macroscopic convection. In almost all the previous theoretical or experimental studies of enhancement in heat transfer in flowing suspensions, the predicted or observed enhancement is attributed to the bulk shearing of the suspension near the walls of the tube. This bulk shear induces individual particle rotation and micro-convection [4].

A very similar effect on the heat transfer mechanism is expected in suspensions which are stationary but in which particles are continuously settling because of the presence of body forces. These motions, which are purely translatory in nature, are also present in flowing suspensions but their effect on the heat transfer mechanisms has not been studied in the literature. The main purpose of the present work is to study the effect of pure translation of particles on the microscopic heat transfer in a monodisperse suspension. Non-affine translation of suspended particles in a flowing suspension (i.e. relative motion between the particles and the fluid) will result in particle migration and will influence the momentum and heat transport mechanisms.

For example, in a suspension of spheres sedimenting in an unbounded, quiescent Newtonian fluid, as the particle volume fraction (ε) increases, hydro-

---

† Author to whom correspondence should be addressed.

dynamic interactions between particles increase resulting in a distribution of diminished particle fall velocities which exhibit *non-zero* variance. The results of our experiments performed on a dilute [$\varepsilon \sim O(10^{-5})$, inter-particle distance $\sim O(40 \times$ particle diameter)], monodisperse homogeneous, non-Brownian suspension of glass spheres 22 μm in size in water using laser doppler anemometery (LDA) show that the particle fall velocity exhibits a standard deviation of more than 30% of the mean value [5]. The effect of distributed fall velocities on the enhanced heat transfer occurring in a sedimenting suspension has not been investigated so far. This research is focused on studying these issues using a reasonable physical model which can give insight into the complex process of heat transfer as it occurs in a monodisperse suspension.

From the available literature it is apparent that there is no reported experimental work which specifically focuses on enhanced heat transfer in suspensions caused by the effect of relative motion between the suspended particles and the suspending fluid.

In this paper we have introduced a simplified model of the complex process of heat transport in a monodisperse suspension in which suspended particles exhibit non-affine motion. To begin with, the suspension as a whole is assumed to be stationary. This simplification with certain assumptions leads to a unit cell model which paves the way for a tractable numeri-

cal scheme which can account for the convective as well as the diffusive heat transport mechanisms at a microscopic scale of the suspended particle. The steady-state solution of the energy equation obtained in this manner leads to the steady-state temperature distribution and thermal flux across the unit cell as a function of suspension parameters such as solid volume fraction and particle Péclet number. The thermal flux across the unit cell is shown to be a function of modified Péclet number that includes the influence of volume fraction for the range of volume fractions $(0 < \varepsilon < 0.3)$ and for $Pe \sim O(1)$. The correlation between the modified Péclet number and the thermal flux is shown to be a simple polynomial which is then used to investigate the influence of distributed particle fall velocities on the estimated heat transfer.

2. THEORY

To illustrate the role of the relative motion between the fluid and the solid inclusion in enhancement of the heat transfer, and to establish that there will be a fundamental change in the mechanism of heat transport, consider the following example. Suppose a particle of diameter $2a$ is moving in a quiescent fluid (subscript 1) which has thermal diffusivity α_1. Time t, required for heat to diffuse a distance of $2a$ in this fluid is given as

$$t_1 \sim O\left(\frac{(2a)^2}{\alpha_1}\right). \tag{1}$$

If the particle has a speed u, time t_2, taken by particle to translate a distance of $2a$, is of the order of,

$$t_2 \sim O\left(\frac{2a}{u}\right). \tag{2}$$

If it is further assumed that the fluid and the particle have identical thermal diffusivities, then on a length scale of the particle diameter, augmentation in heat transfer will be of significance provided, $t_1/t_2 \geqslant 1$. The ratio of the time values is the Péclet number, based on the particle diameter, its relative velocity with respect to the suspending fluid and the fluid diffusivity. Thus, it is this non-dimensional quantity that governs or dictates the dominance of convective heat transfer due to particle motion over purely conductive heat transfer which occurs in quiescent fluid. Whenever $Pe \geqslant 1$, it is necessary to account for convective effects in a suspension.

Dimensional analysis reveals that heat transfer across such suspensions is governed by particle Péclet number ($Pe = UL/\alpha_1$), the ratio of thermal diffusivities of the fluid and the particle and the ratio of thermal conductivities of the two phases and particle volume fraction. Here, L is a characteristic length scale which is related to particle size through volume fraction of the suspension.

Normally, if the entire suspension is deformed, it is difficult to characterize the magnitude of the relative motion between the suspended particles and the suspending fluid. This characterization can be done for a quiescent, *unbounded* suspension of hard spheres in a Newtonian fluid such as water. Here the term *unbounded* is used in the sense that the ratio of container dimension to particle diameter is sufficiently large (> 1000), so one can justifiably neglect wall effects. These hard spheres may then be allowed to settle in the medium creating non-affine motion because of body forces such as the gravitational field. By selecting the quiescent medium, convective flux due to bulk motion of the fluid under consideration is eliminated and allows one to focus attention on enhanced heat transfer occurring solely because of particle induced micro-convective heat transfer.

2.1. Governing equations

In order to construct a tractable mathematical model for the prediction of heat transfer in such monodisperse suspensions, a number of simplifications are made. If the flow is steady and sufficiently slow that the inertial and turbulent effects are ignored, only the pressure and viscous terms need be retained in the momentum equations: the incompressible continuity equation remains the same. Thus the governing equations for the solution of Stokes problem are [6]

$$\nabla \cdot \mathbf{u} = 0 \tag{3}$$

$$0 = -\nabla p + \mu \nabla^2 \mathbf{u} \tag{4}$$

where $\mathbf{u}$ is the velocity of the fluid, p is the pressure and μ is the fluid viscosity.

Furthermore, it is assumed that a steady-state temperature field exists on the macroscopic scale throughout the domain under consideration and thus one needs to solve after neglecting viscous dissipation, only the steady-state energy equation, which is

$$Pe\,\mathbf{u} \cdot \nabla T - \nabla^2 T = 0. \tag{5}$$

In equation (5), $\mathbf{u}$ is the fluid or particle velocity, Pe is the Péclet number and T is the temperature. Here the Péclet number is based on particle speed U, characteristic length scale L based on the average particle separation and thermal diffusivity α, which can be expressed as

$$Pe = \frac{UL}{\alpha} \quad \text{where} \quad \alpha = \frac{k_1}{(\rho C_p)_1} \text{or} \frac{k_2}{(\rho C_p)_2} \tag{6}$$

depending on whether the point under consideration belongs to the fluid (subscript 1) or the solid portion (subscript 2) of the suspension. At the interface of the two phases, the temperature and the energy flux are assumed to be continuous. For this analysis, we assumed thermal conductivities, and heat capacities of the fluid and the particle to be identical.

2.2. Model simplification

For the sake of simplicity and to provide a viable model, this dispersion is assumed to be homogeneous and consisting of regular periodic arrays of particle centers translating in a fixed coordinate direction with respect to the bulk suspension which is stationary. This condition needs to be met in a region of space at length scales much larger than the particle diameter, which may be called a 'sub-domain' as shown in Fig. 1. This enables one to study heat transfer across a single particle located in a cubic unit cell in a given sub-domain characterized by: a particle volume fraction; a local particle Péclet number in which the length scale is the diameter of the unit sphere; and a specified temperature or flux boundary condition. Within this unit cell, because of relative motion between the particle and the fluid, the induced disturbance in the fluid velocity can be modeled in a variety of ways and can be coupled with the energy equation to investigate the heat transfer across this cell. These results would be valid for the sub-domain under consideration.

As an assemblage of particles moves through an unbounded fluid, it creates a velocity field throughout the fluid. This velocity field consists of fluid which is being dragged by the moving particles and the fluid moving in the opposite direction, as it is displaced by the particle. As a result of these motions, it is expected that the rate of heat transfer in a moving dispersion may differ considerably from that in a stationary dispersion. The complexities involved have prevented analytical treatment in the literature.

A closely related process to this problem is sedi-

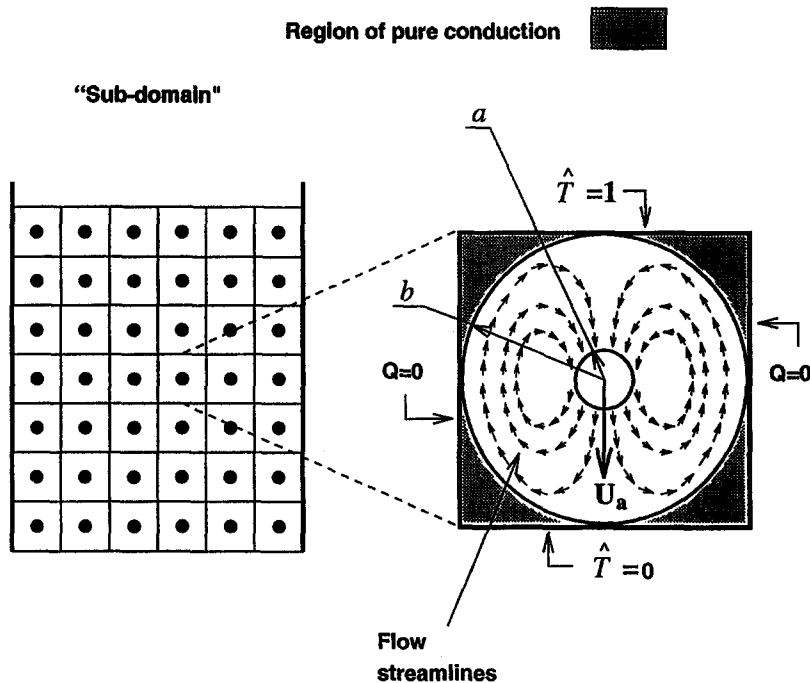**Region of pure conduction** ▉

"Sub-domain"

Fig. 1. Schematic of unit cell model.

mentation, where particles fall under the action of gravity through a fluid in which they are suspended. This occurs in many natural processes as well as in important separation processes used in the chemical industry. It was also pointed out earlier that these fall velocities show a large standard deviation about the mean value due to the hydrodynamic interactions.

To investigate the dependence of the rate of heat transfer on this standard deviation in a settling dispersion, it is essential to simplify the complex boundary value problem involving many particles. In this numerical work, to make the problem tractable, the unit cell method is used. The unit cell method relies on the concept that an assemblage may be divided into a number of identical cells, one particle occupying each cell. This allows one to simplify the boundary value problem by considering the boundary of a single particle and its bounding volume. Although this technique is restricted to suspensions in which particles are moving in regular periodic arrays, its results can be applicable to random arrays in some stochastic sense [7].

3. UNIT CELL APPROACH

To predict numerically the effective heat flux across a horizontal plane in an unbounded dispersion of rigid spheres and its dependence on average particle velocity relative to the medium, the *unit* cell technique is used. This technique is based on the concept that an assemblage of spherical particles can be divided into a number of identical cubic or spherical cells with one particle occupying each cell. Naturally, this

technique is limited only to regular periodic arrays of moving particles with identical size and material properties. The use of this technique and the assumption about the configuration of the particles as they fall, allows one to reduce the complex boundary value problem involving numerous interacting particles to a single unit cell containing a single particle and suitable boundary conditions applied on the unit cell and particle surfaces to account for and closely model real dispersions.

To simulate heat transfer across a plane in such a dispersion which is unbounded, any proposed unit cell model must be able to account for:

(a) conductive heat flux due to an imposed temperature gradient which is same as the macroscopic temperature gradient,

(b) convective heat flux due to the motion of the particle and the fluid which is dragged along with it, and

(c) convective heat flux due to the motion of fluid in the opposite direction to the particle motion which is displaced because of the moving particle and the accompanying fluid so that the condition that total volumetric flux across any plane perpendicular to the direction of motion is *zero* is met.

The unit cell selected is a unit cube with a spherical particle at the center of the cell as shown in Fig. 1. A temperature gradient is imposed which coincides with the z-coordinate direction. The volume fraction of the suspended particles decides the diameter of the spherical particle. This particle is assigned a velocity in the negative z-coordinate direction which generates

a flow field in the surrounding fluid. It is possible to find the flow field numerically, but in this study, to take advantage of the existing analytical solution for the flow field around a spherical particle, a fictitious spherical envelope of fluid surrounding the particle is assumed. This envelope is concentric with the spherical particle and its diameter is equal to the length of the unit cell. By imposing appropriate boundary conditions on the surface of the particle and on the surface of this envelope and using stream-function formulation in spherical coordinates, a steady-state flow field inside the spherical unit cell is obtained, the details of which are given in the next section. According to Happel and Brenner [7], the motion of a sphere at the instant it passes the center of a spherical container is assumed to emulate the importance of wall effects in the motion of a single particle, in addition to providing a model of interactions among particles in unbounded multiparticle systems. We hypothesize that the same assumption holds for extracting information about micro-convection effects on the overall heat transfer occurring in a unit cell. It is further assumed that each particle acts as an independent source for microscopic heat and mass transfer at its spatial location as it translates through the fluid. This allows one to obtain a correlation between the particle speed and the heat flux across the unit cell by studying the steady-state temperature field within the unit cell at the instant when the particle passes through the center of the cell. The justification for the solution the steady-state temperature field is not entirely obvious. Firstly, it is supported by the assumption that the steady state has been achieved at the macroscopic length scale. The implication of the first assumption is that the location of the particle within the representative unit cell is inconsequential for the heat flux in the direction of applied temperature gradient. Thus we select the particle location which coincides with the center of the unit cell. Secondly, we solve for flow using equation (4), which gives a solution which is *quasi-steady*. This means that as the particle translates through the fluid, the flow field also translates with it instantaneously, justifying the use of the steady-state temperature field to obtain heat flux across the unit cell.

3.1. Flow field inside a spherical unit cell

Let us suppose that a solid sphere of radius a is held fixed with its center coinciding with the center of a spherical coordinate system in an otherwise uniform stream of fluid. Let us further assume that the disturbance in the uniform fluid flow caused by the presence of this sphere is restricted within a concentric spherical envelope of radius b. The spherical coordinate system used is shown in Fig. 2, and the $\theta = 0$ direction is chosen to coincide with the uniform fluid flow (or particle velocity) direction. Because of the axisymmetric nature of the problem, the choice of the $\phi = 0$ direction is unimportant. Thus the creeping flow past this sphere is a planar flow in spherical

coordinates which can be described completely by velocity components v_r and v_θ in the r and θ directions respectively. For particle Reynolds number $Re_p \leqslant 0.1$, the governing equations are still the same (equations (3) and (4)), and the flow field can be obtained using the stream function formulation.

Assuming v_r and v_θ of the following form

$$v_r = \frac{1}{r^2 \sin \theta} \frac{\partial \psi}{\partial \theta} \quad \text{and} \quad v_\theta = -\frac{1}{r \sin \theta} \frac{\partial \psi}{\partial r} \quad (7)$$

where

$$\psi(r, \theta) = \tfrac{1}{2} U f(r) \sin^2 \theta \quad (8)$$

is the stream-function in spherical coordinates and U is the free stream velocity of the fluid at $r = b$. It has been shown [7] that this formulation reduces to solving the following equation for $\psi(r, \theta)$, namely,

$$\nabla^4 \psi = 0. \quad (9)$$

It can be further shown that $f(r)$ has the following form:

$$f(r) = \frac{A}{r} + Br + Cr^2 + Dr^4. \quad (10)$$

It is to be noted that the unknown flow field being sought is in the region of space between the particle surface and the outer envelope and hence,

$$a \leqslant r \leqslant b \quad \text{or equivalently} \quad a \leqslant r \leqslant \frac{a}{\lambda} \quad (11)$$

condition applies for the entire analysis, where $\lambda = a/b$ is a dimensionless parameter with the following restriction,

$$0 < \lambda < 1. \quad (12)$$

This formulation appears in many standard texts on the subject such as Happel and Brenner [7]. The problem reduces to finding out different *sets* of four constants A, B, C and D corresponding to chosen *sets* of four boundary conditions. In this work, two different sets of boundary conditions will be used to obtain two different velocity fields to evaluate the sensitivity of the final results on the type of boundary conditions or flow field used.

3.1.1. Boundary conditions I. To allow comparison with the special case of a more general result pertaining to translation of two concentric fluid spheres, this set of boundary conditions is such that the inner sphere is held at rest and the outer envelope is moved with speed U coinciding with the $\theta = 0$ direction. By subtracting U from the velocity field so obtained, we get the desired velocity field where the particle translates with the velocity U in a quiescent fluid. The present boundary conditions can be stated as:

$$v_r = U \cos \theta \quad \text{and} \quad v_\theta = -U \sin \theta \quad \text{at} \quad r = b$$
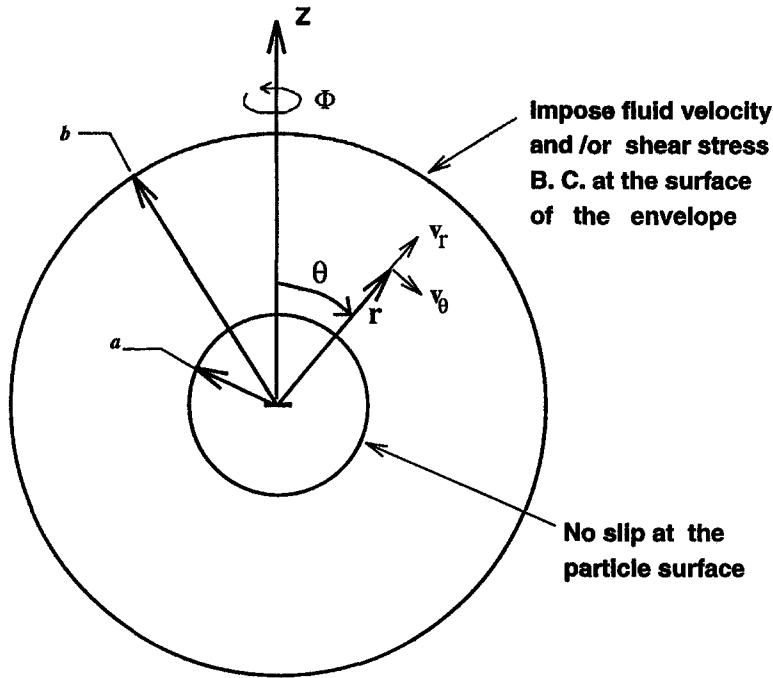
$$(13)$$

and

Fig. 2. Spherical coordinates used to obtain the flow field.

$$\frac{\partial \psi}{\partial r}\bigg|_{r=a} = \frac{\partial \psi}{\partial \theta}\bigg|_{r=a} = 0. \qquad (14)$$

Boundary conditions in equation (13) enforce free stream fluid velocity at the surface of the spherical unit cell and those in equation (14) enforce *no slip* at the surface of the particle. These four boundary conditions yield a set of four algebraic equations involving two known parameters, namely a and λ, and four constants A to D which are unknowns. After lengthy algebra and simplification, the following expressions have been obtained for constants A to D:

$$A = a^2 B + 2a^3 C + 4a^5 D$$

$$B = -\frac{3}{2}aC - \frac{5}{2}a^3 D$$

$$C = \frac{(9\lambda^4 + 9\lambda^3 + 4\lambda^2 + 4\lambda + 4)}{(1-\lambda)^3(4\lambda^2 + 7\lambda + 4)}$$

$$D = \frac{3\lambda^3(2\lambda^4 + 6\lambda^3 + 10\lambda^2 + 9\lambda + 3)}{a^2(1-\lambda)(-2\lambda^5 + 5\lambda^2 - 3)(4\lambda^2 + 7\lambda + 4)}. \qquad (15)$$

Now, using equations (7), (8) and (15) one can express $v_r(r, \theta)$ and $v_\theta(r, \theta)$ as:

$$v_r = U\cos\theta\left[\frac{A}{r^3} + \frac{B}{r} + C + Dr^2\right] \qquad (16)$$

and

$$v_\theta = U\sin\theta\left[\frac{A}{2r^3} - \frac{B}{2r} - C - 2Dr^2\right]. \qquad (17)$$

Verification of the flow field. Since the algebra involved in the computation of constants A to D is cumbersome, it is important to see that the results

reduce to Stokes solution for flow past a stationary sphere in an unbounded medium. In the above analysis, as $b \to \infty$, $\lambda \to 0$, and one should obtain Stokes solution; thus, as can be readily seen from equations (15), as $\lambda \to 0$,

$$D \to 0$$

$$C \to 1$$

$$B \to -\frac{3}{2}a$$

$$A \to \frac{a^3}{2}$$

which is a *benchmark* solution available in the literature.

To verify that the enforced boundary conditions are satisfied, using equations (16) and (17), functions $v_r/U\cos\theta$ and $v_\theta/U\sin\theta$ were plotted against r for various values of the parameters a and λ. It is found that for a wide range of values of the parameters used, the boundary conditions at $r = a$ and $r = b$ are satisfied in each and every case. To compare the intermediate values (for $a < r < b$) of the above two functions, the solutions given by Happel and Brenner [7] for two concentric spheres in relative motion for a special case of rigid inner sphere were chosen. The results obtained here match very well with the special case given by Happel and Brenner.

3.1.2. *Boundary conditions II.* The boundary conditions for this case where the suspending medium is at rest and a spherical particle is moving with speed U in the $\theta = 0$ direction can be stated as:

$$v_r = U\cos\theta \quad \text{and} \, v_\theta = -U\sin\theta \quad \text{at} \, r = a, \qquad (18)$$

and

$$v_r = 0 \quad \text{and} \frac{\partial v_\theta}{\partial r} - \frac{v_\theta}{r} = 0 \quad \text{at } r = b. \qquad (19)$$

Here the boundary conditions selected are the ones used by Happel [8], in the so-called 'free surface' model where on the surface of the spherical envelope, the shear stress $\tau_{r\theta}$, and v_r components of fluid velocity are set to zero (equation (19)) instead of imposing free stream fluid velocity as in the previously stated boundary conditions (refer to equation (13)). The corresponding constants for these boundary conditions are as follows:

$$A = -\frac{a^3}{(2-3\lambda+3\lambda^5-2\lambda^6)}$$

$$B = \frac{a(3+2\lambda^5)}{(2-3\lambda+3\lambda^5-2\lambda^6)}$$

$$C = -\frac{\lambda(3+2\lambda^5)}{(2-3\lambda+3\lambda^5-2\lambda^6)}$$

$$D = -\frac{\lambda^5}{a^5}A. \qquad (20)$$

Once again, using equations (7), (8) and (20) one can express $v_r(r,\theta)$ and $v_\theta(r,\theta)$ as:

$$v_r = U\cos\theta\left(\frac{A}{r^3}+\frac{B}{r}+C+Dr^2\right) \qquad (21)$$

and

$$v_\theta = U\sin\theta\left(\frac{A}{2r^3}-\frac{B}{2r}-C-2Dr^2\right). \qquad (22)$$

These velocities have been numerically verified and they do satisfy the boundary conditions stated in equations (18) and (19) for a wide range of values of the parameters a and b or λ.

To decide which flow field best represents the physics more realistically, we compare the two flow fields as well as the shear fields obtained by imposing boundary conditions I and II. The plots of $v_r/U\cos\theta$, $v_\theta/U\sin\theta$ and $\tau_{r\theta}/U\mu\sin\theta$ which are shown in Figs. 3, 4 and 5 for the two types of boundary conditions are compared. For simplicity we have chosen $a = 1$ and $b = 2$, which meet the condition $a < b$. It is to be noted that shear fields for both the flow fields are given by

$$\frac{\tau_{r\theta}}{\mu U\sin\theta} = -\frac{3A}{r^4}-3Dr \qquad (23)$$

provided respective sets of constants are used.

In order to ensure a valid comparison, the solution for the first set of boundary conditions has been modified by subtracting the velocity of the envelope and changing the sign of the velocity. This describes the situation where a particle moves with the velocity U

in the z direction and the envelope is stationary, which is identical to the physical situation for the second set of boundary conditions. From Fig. 3, which compares the radial component of fluid velocity, it can be seen that at $r = 2(= b)$, because $v_r = 0$, for both the flow fields there is no mass transfer across the outer envelope. From Fig. 4, which compares the tangential component of fluid velocity, in which $v_t \neq 0$ at $r = 2(= b)$ for the second flow field. However, from Fig. 5 it can be seen that shear stress $(\tau_{r\theta})$ is zero as enforced by the second set of boundary conditions, but it is not zero for the first flow field. Thus the second set of boundary conditions is superior to the first set of boundary conditions as there is no mass or momentum transfer taking place across the outer envelope. This justifies the use of the flow field obtained using the second set of boundary conditions in the energy equation.

3.2. Governing energy equation

To investigate steady state heat transfer across the unit cell under consideration, it is necessary to solve for a steady-state temperature field inside the unit cell. We begin with non-dimensionalizing the temperature using temperatures T_1 and T_2, which are bottom and top face temperatures of the unit cell. Thus, non-dimensionalized temperature $\hat{T}$ can be written as:

$$\hat{T} = \frac{T-T_1}{T_2-T_1}. \qquad (24)$$

Since this study is focused on the influence of pure convection on the heat transfer, the physical properties of the fluid and the spherical particle (thermal conductivity and thermal diffusivity) are assumed to be identical.

Furthermore, if the Brinkman number for the process, $Br = \mu U^2/(k_1|T_2-T_1|) \ll 1$, one can neglect viscous dissipation terms and then the non-dimensionalized steady-state energy equation can be stated as [9]:

$$Pe\,\mathbf{u}\cdot\nabla\hat{T}-\nabla^2\hat{T} = 0. \qquad (25)$$

In Equation (25), $\mathbf{u}$ is the fluid or particle velocity, Pe is the Péclet number and $\hat{T}$ is the non-dimensionalized temperature as defined in equation (24). Here the Péclet number ($= UL/\alpha_1$) is based on particle speed U and the length of the unit cell L. The length scale L is related to particle radius a through particle volume fraction ε which is defined as

$$\varepsilon = \frac{4\pi}{3}\left(\frac{a}{L}\right)^3. \qquad (26)$$

4. NUMERICAL SCHEME

The unit cell under consideration is discretized in three Cartesian directions so that node numbers (i, j, k) correspond to the x, y and z directions respectively. Because of the symmetry of the problem about
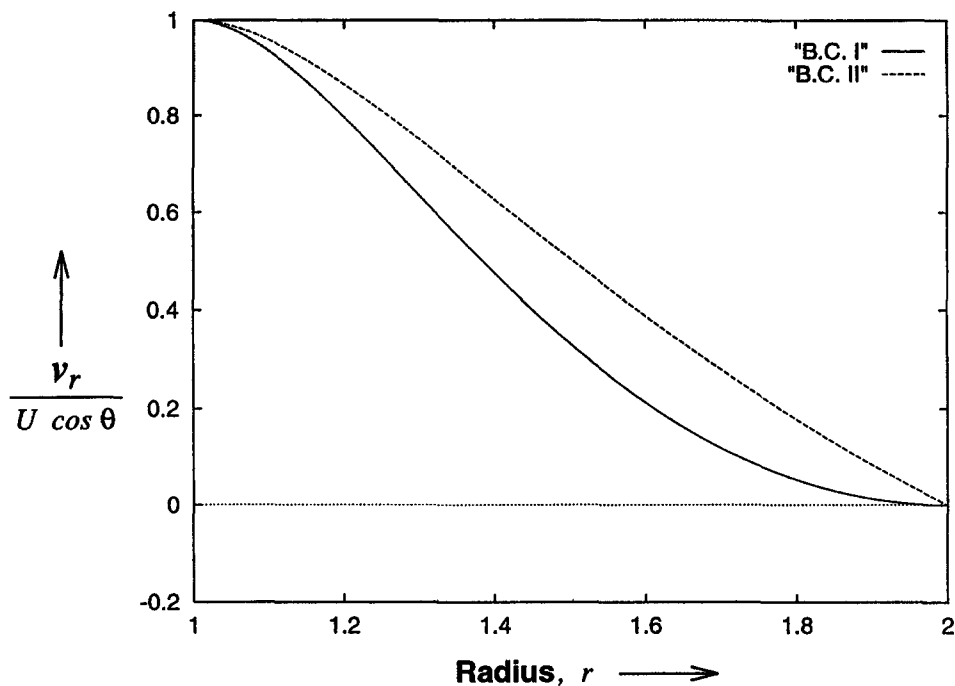
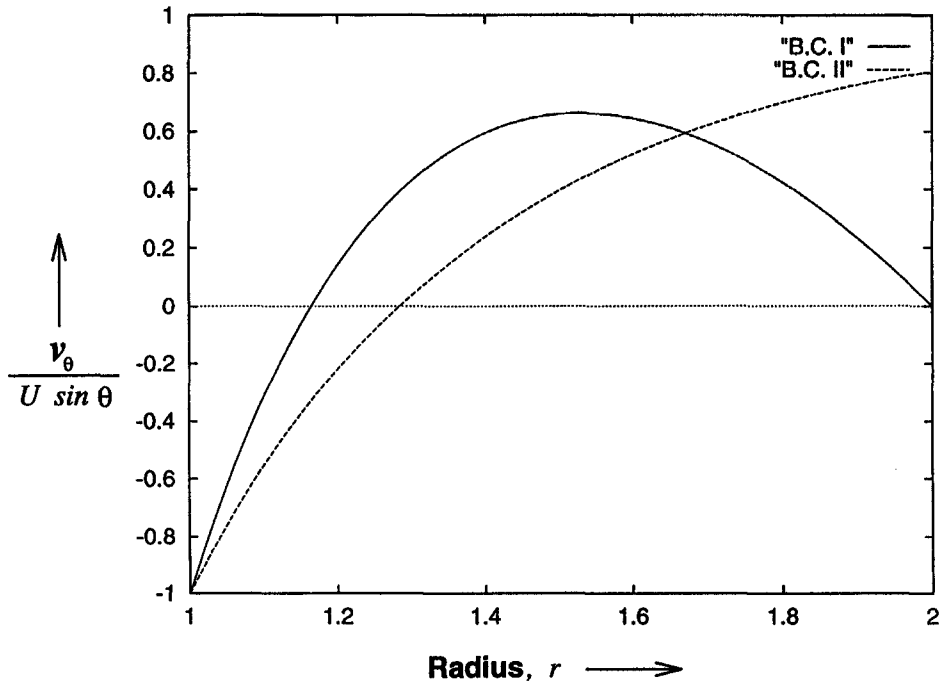Fig. 3. Comparison of radial velocity for flow fields I and II.

Fig. 4. Comparison of tangential velocity for flow fields I and II.

the z axis, the choice of x and y directions is immaterial and the solution is sought only in one quarter of the unit cell. The energy equation (equation (25)) is discretized using the control volume approach which gives an algebraic equation (conservation of energy) at each spatial node. For a node which is completely
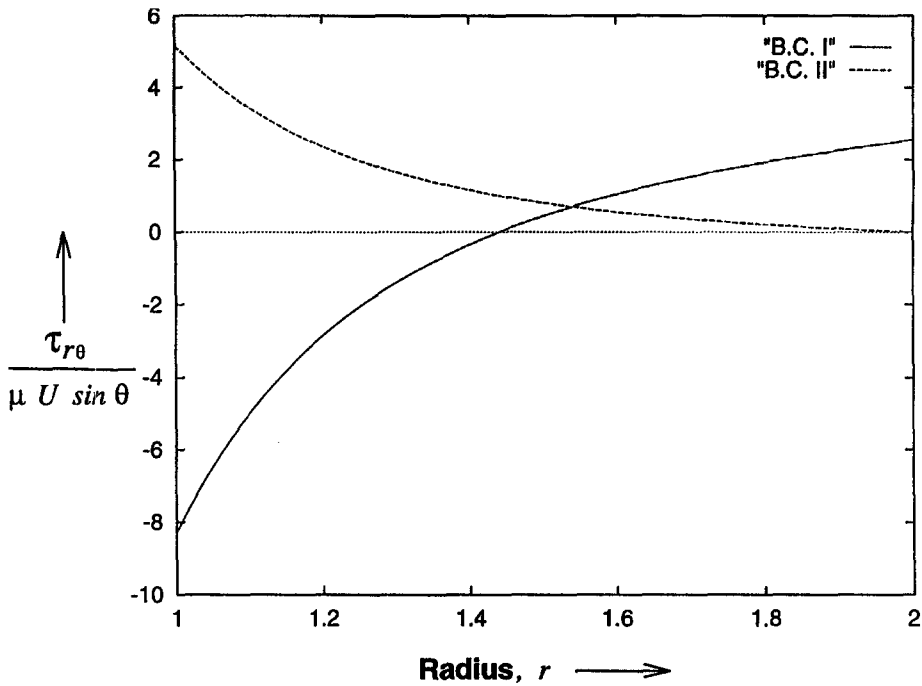
Fig. 5. Comparison of shear stress for flow fields I and II.

surrounded by fluid, this discretization can be stated as:

$$Pe[u(i-1,j,k)\hat{T}(i-1,j,k)$$

$$-u(i+1,j,k)\hat{T}(i+1,j,k)]\frac{\Delta y\Delta z}{2}$$

$$+Pe[v(i,j-1,k)\hat{T}(i,j-1,k)$$

$$-v(i,j+1,k)\hat{T}(i,j+1,k)]\frac{\Delta z\Delta x}{2}$$

$$+Pe[w(i,j,k-1)\hat{T}(i,j,k-1)$$

$$-w(i,j,k+1)\hat{T}(i,j,k+1)]\frac{\Delta x\Delta y}{2}$$

$$=\left[\frac{\hat{T}(i,j,k)-\hat{T}(i-1,j,k)}{\Delta x}\right.$$

$$\left.-\frac{\hat{T}(i+1,j,k)-\hat{T}(i,j,k)}{\Delta x}\right]\Delta y\Delta z$$

$$+\left[\frac{\hat{T}(i,j,k)-\hat{T}(i,j-1,k)}{\Delta y}\right.$$

$$\left.-\frac{\hat{T}(i,j+1,k)-\hat{T}(i,j,k)}{\Delta y}\right]\Delta z\Delta x$$

$$+\left[\frac{\hat{T}(i,j,k)-\hat{T}(i,j,k-1)}{\Delta z}\right.$$

$$\left.-\frac{\hat{T}(i,j,k+1)-\hat{T}(i,j,k)}{\Delta z}\right]\Delta x\Delta y. \qquad (27)$$

This equation is identical for spatial locations either

in the fluid or solid portion of the unit cell because thermal properties have been assumed to be identical here. However, for all the nodes belonging to the solid portion, the imposed velocity is simply $(0,0,-U)$, which is the particle velocity. This algebraic equation (equation (27)) consists of known fluid velocity components from equations (21) and (22), and unknown temperatures at the node under consideration and the surrounding six nodes as well. As shown in Fig. 1, a steady-state temperature gradient is assumed in the vertical direction in a sedimenting suspension which is unbounded in the horizontal direction. This leads to the temperature and flux boundary conditions which have been applied on the six faces of the unit cell under consideration. These conditions are $\hat{T} = 1$ at the top face, $\hat{T} = 0$ at the bottom face and heat flux $Q = 0$ at all the four remaining vertical faces of the unit cell. Using successive substitution, imposed boundary temperatures are 'numerically diffused' throughout the unit cell until a steady-state temperature distribution is obtained. Using this temperature distribution, energy flux is computed at the top and the bottom face of the unit cell by 3-point asymmetric finite-difference schemes to approximate thermal gradients at the node under consideration. For the bottom face $(z = 0)$ on which $k = 1$, the 3-point asymmetric forward difference is used as follows,

$$\frac{\mathrm{d}\hat{T}}{\mathrm{d}z}(i,j,1) = \frac{-1.5\hat{T}(i,j,1)+2.0\hat{T}(i,j,2)-0.5\hat{T}(i,j,3)}{\Delta z}. \qquad (28)$$
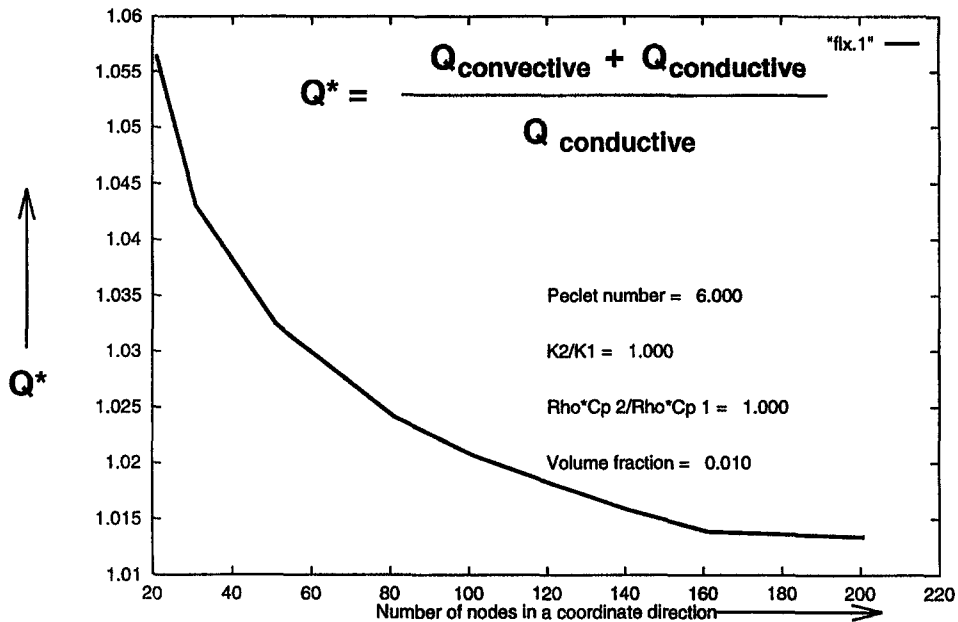
Fig. 6. A typical convergence study for the numerical scheme.

For the top face $(z = L)$ on which $k = K_{max}$, the 3-point asymmetric backward difference is used as follows [10],

$$\frac{d\hat{T}}{dz}(i,j,K_{max}) = \frac{1.5\hat{T}(i,j,K_{max}) - 2.0\hat{T}(i,j,K_{max}-1)}{\Delta z} + 0.5\hat{T}(i,j,K_{max}-2)}{\Delta z}.$$

(29)

These energy fluxes should be identical for this case because there is no flux boundary condition at the four vertical faces of the unit cell. This provides an additional check on the accuracy of the numerical technique. This flux is non-dimensionalized as follows:

$$Q^* = \frac{Q_{convective} + Q_{conductive}}{Q_{conductive}}.$$

(30)

In the definition of Q^*, $Q_{conductive}$ denotes the conductive flux across any horizontal plane of the unit cell in the absence of fluid motion, i.e. for the case when $Pe = 0$ and all other boundary conditions are identical. Thus Q^* is an appropriate measure of enhanced heat transfer across the unit cell.

To ensure correctness of the numerical scheme, a flow field $(u = 0, v = 0, w = \text{constant})$ was imposed within the unit cell with the same temperature and flux boundary conditions on the unit cell as stated earlier. The analytical solution for the steady-state temperature distribution within the unit cell for this case compared well with the numerical solution. Furthermore, convergence of this numerical scheme has been verified by mesh refinement for many different volume fractions as well as Péclet numbers. A typical plot of convergence of Q^* vs number of nodes in a coordinate direction is shown in Fig. 6.

5. RESULTS

For all the cases studied, the flow field obtained using the second set of boundary conditions (refer to Section 3.1.2) is used. This flow field is more consistent with the unit cell model in which the fluid outside the outer envelope is stationary. It was also found that if the flow field obtained using the first set of boundary conditions were used, then the Q^* values did not differ by more than $+3\%$ as compared with the values in Fig. 7. In all 162 cases were simulated for Péclet numbers 0–17 for nine different volume fractions which were 0.001, 0.002, 0.003; 0.010, 0.020, 0.030; 0.100, 0.200 and 0.300. The results of these simulations are shown in Fig. 7. It is to be noted that these results are valid even at a high volume fraction of 0.300 simply because the resulting higher particle interactions have been taken care of by confining the flow disturbance within the spherical unit cell. For volume fractions greater than about 0.350, the present numerical scheme becomes unstable because of the sharp rise in the magnitude of discontinuity in the v_θ component of velocity at the outer spherical envelope (see Fig. 4).

From the graphs in Fig. 7, it is clear that the rate of heat transfer increases monotonically with the cell Péclet number for all ranges of volume fractions. The enhancement is negligible whenever $Pe < 1$. Also for lower volume fractions $(\varepsilon \leqslant 0.003)$, the enhancement is negligible irrespective of the Péclet number for the range covered here. It is also apparent from the graphs that the enhancement increases monotonically with the volume fraction and becomes non-linear as the volume fraction increases. Also the degree of non-linearity increases with volume fraction. However, it is important to note that the monotonic increase in Q^*
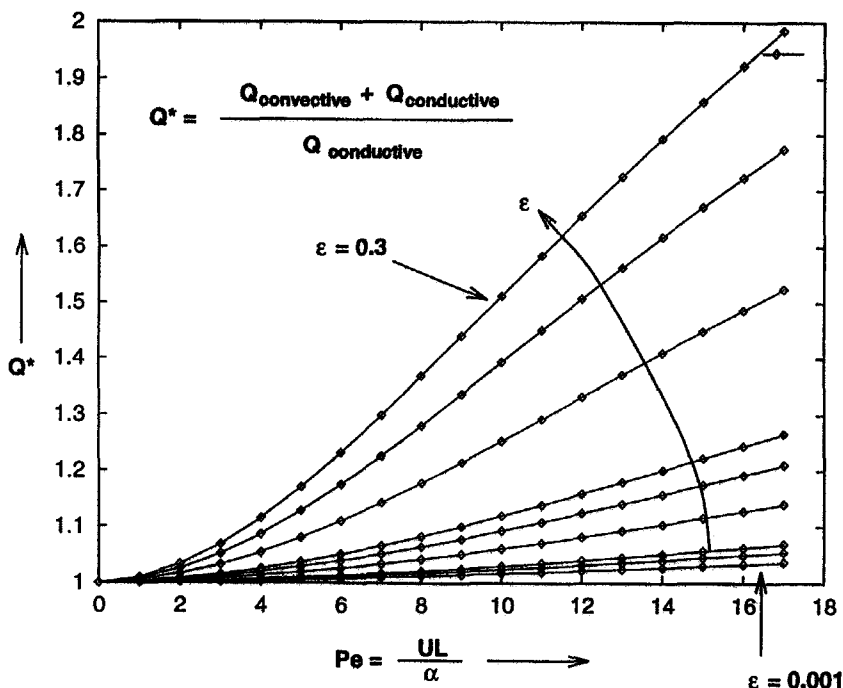
Fig. 7. Effective heat flux vs Péclet number for a range of volume fractions.

with ε will not continue indefinitely as the temperature gradients at the unit cell wall are bounded by the analytical solution for the cases when the entire fluid in the cubic unit cell moves with the velocity components $u = 0$, $v = 0$ and $w = \pm$ (non-zero constant).

5.1. Introduction of a modified Péclet number

In order to see if the results of Fig. 7 could be collapsed together, a numerical search was conducted to find out a physical parameter that would collapse all the 162 case studies. Since there are only two parameters, namely the Péclet number and the volume fraction, describing the system, their proper combination would be able to correlate the results. It should be emphasized here that inter-particle distance, L, and particle volume fraction, ε, are correlated for a fixed particle radius, a, as can be seen from equation (26). Thus, for a fixed particle size, the Péclet number can be scaled using the volume fraction ε. By introducing a modified Péclet number,

$$Pe' = Pe \times \varepsilon^{3/4} \qquad (31)$$

a clear collapse of the numerical results was achieved as depicted in Fig. 8. This indicates that enhanced heat transfer can be related to the modified Péclet number for the range of volume fractions investigated here. This allows us to relate enhanced heat transfer to modified Péclet number using a fourth-order polynomial which can be useful in a variety of ways for process modeling and development. The polynomial can be stated as:

$$Q^*(Pe') = f(Pe') = 1.000 + 0.0556 Pe'$$

$$+ 0.1649 Pe'^2 - 0.0391 Pe'^3 + 0.0034 Pe'^4. \qquad (32)$$

How a simple polynomial relationship between heat transfer across a unit cell and modified Péclet number can be useful is illustrated in Section 5.2.

5.2. Explanation for modified Péclet number

Various scaling laws and the possibility of using perturbation analysis to explain equation (31) quantitatively were explored. Scaling laws oversimplify the 3-D problem at hand and a perturbation expansion in ε (which is a parameter) for the temperature distribution would require solving zeroth-, first- and higher-order problems numerically because of the complex 3-D domain. Thus, what follows in the next paragraph is an attempt to explain equation (31) qualitatively.

The results of the numerical case studies as well as the existence of the modified Péclet number suggest that there exists a characteristic velocity other than U which is related to the volume fraction in some manner for the present configuration. A simple analysis which is valid for cylindrical geometry can give some clues to this characteristic velocity. If an elemental disc of radius a is assumed to be translating with a z-velocity of $-U$, then the average velocity of the fluid in the surrounding envelope is

$$\bar{U} = \left(\frac{a^2}{1-a^2}\right)U. \qquad (33)$$

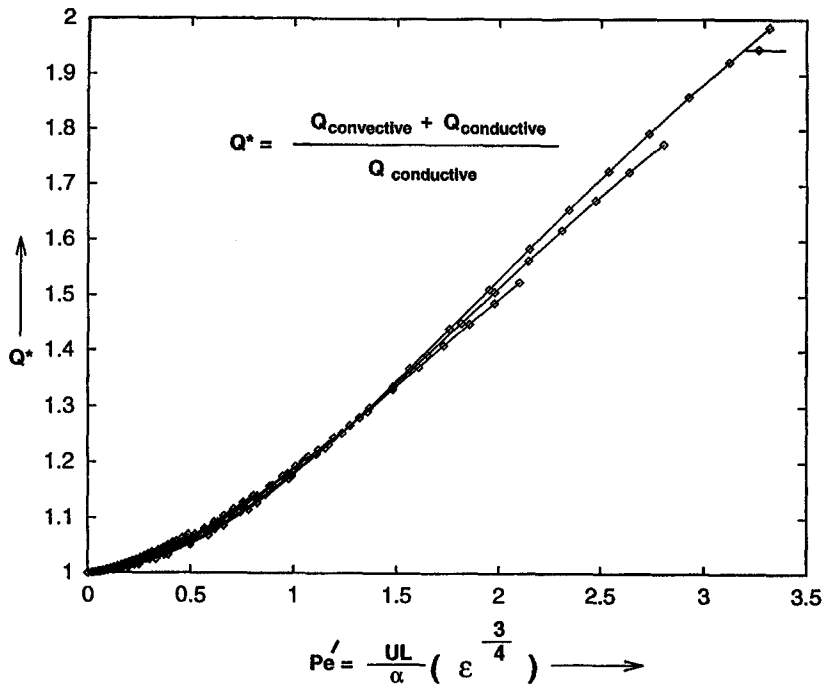This would modify the cell Péclet number as

Fig. 8. Effective heat flux vs modified Péclet number for a range of volume fractions.

$$Pe' = \frac{UL}{\alpha} \times \frac{\bar{U}}{U}$$

$$= Pe\left(\frac{a^2}{1-a^2}\right)$$

$$\sim Pe(\varepsilon^{2/3} + \varepsilon^{4/3} + \varepsilon^2 + \varepsilon^{8/3} + \cdots). \qquad (34)$$

Thus it can be seen that the average velocity of the fluid in the annulus surrounding the falling disc could be the characteristic velocity for the convective heat transfer which occurs at low volume fractions. Although this oversimplifies the 3-D heat transfer that occurs because of the motion of a spherical particle inside the unit cell, it supports our view that heat transfer in the 3-D unit cell is characterized by a velocity other than U.

5.3. *Effect of distributed velocities on enhanced heat transfer*

So far the discussion was based on the Péclet number which is assumed to be uniform in the unit cell and hence throughout the suspension. Thus the results obtained so far are applicable to unit cells that all have a particle translating at the center with a steady fall velocity and with zero standard deviation. One can apply these results to a suspension of particles which show distributed velocities about a mean fall velocity, to explore how it affects the enhanced heat transfer. For example, if a normal distribution is assumed then, because of the non-linear dependence of Q^* on Pe', the weighted mean of the enhanced heat transfer would be different from the estimate based solely on the average fall velocity of the particles.

For a suspension which has achieved normal particle fall velocity distribution, unit cells will have particles with fall velocities which follow a normal probability density function (p.d.f.). One can estimate the effect of micro-convection on enhanced heat transfer Q^* by finding an average velocity from the distribution of velocities and calculating the average modified Péclet number ($\bar{Pe}'$) based on the average velocity ($\bar{U}$) and using equation (32) to find Q^*, which we denote as $Q^*(\bar{Pe}')$. However, this estimate cannot account for the effect of higher moments of the p.d.f. on enhanced heat transfer due to micro-convection. To incorporate the effect of the distribution function on the overall heat transfer occurring at an average particle fall velocity, we compute a modified Péclet number for each particle velocity and then use either Fig. 8 or equation (32) to find Q^*. The sum of all such Q^*s duly weighed by the p.d.f. for each fall velocity gives us a correct estimate of enhanced heat transfer due to micro-convection and we denote it by $Q^*(\bar{Pe}', \sigma)$. This notation is used here to stress the fact that enhancement depends on $\bar{Pe}'$, the mean modified Péclet number, as well as on σ, the standard deviation or the second moment of the p.d.f.

$Q^*(\bar{Pe}', \sigma)$ accounts for the shape of the p.d.f. as well as the functional form of the polynomial and hence it is the correct estimate. The % error which one must expect if only the average modified Péclet number based on the average particle fall velocity is used is then,

$$\%\text{error} = \left|\frac{Q^*(\bar{Pe}') - Q^*(\bar{Pe}', \sigma)}{Q^*(\bar{Pe}', \sigma)}\right| \times 100. \qquad (35)$$
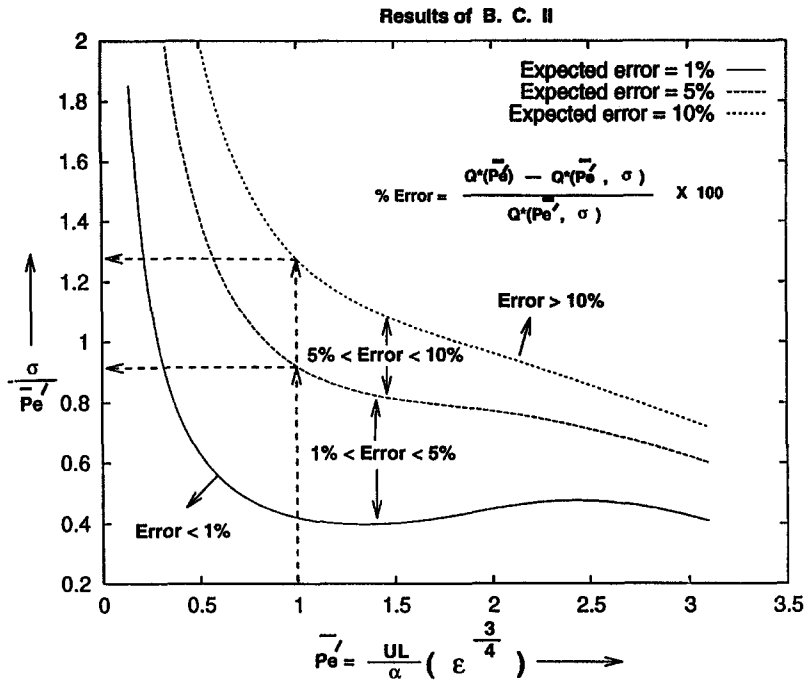
Results of B. C. II

Fig. 9. Regimes of expected % error in the predicted heat flux based on the suspension parameters.

This is illustrated in Fig. 9 where the assumed p.d.f. is a normal distribution and the selected volume fraction is 0.3. On the y axis is the fractional standard deviation of the normal distribution $(\sigma/\bar{Pe}')$. The x axis is the averaged modified Péclet number. The three plots separate the zones in which errors are less than 1, 5 and 10% respectively.

The usefulness of Fig. 9 can be demonstrated by an example where the averaged modified Péclet number $(\bar{Pe}')$ is 1.0. If the particle fall velocities in the suspension show $\sigma/\bar{Pe}' = 0.90$, then the error in the estimated enhanced heat transfer based only on $\bar{Pe}'$ would be 5%. It can also be seen that if the suspension were to have a higher standard deviation of $\sigma/\bar{Pe}' = 1.3$, then the error would be 10% instead of 5%. Thus this diagram is a useful tool for a designer in estimating error based on the suspension parameters.

6. SUMMARY

In a monodisperse suspension of particles showing non-affine motion, micro-convection can play a significant role in the overall heat transfer at a macroscopic scale. In order to test this hypothesis, a simplified process model based on the concept of a unit cell was presented. Inter-particle hydrodynamic interactions were accounted for by confining particle-induced flow disturbance to a spherical envelope of unit diameter. The governing energy equation was solved numerically using a closed form solution for the induced flow field. After testing the accuracy as well as the convergence of the numerical scheme, a range of case studies was performed for low Péclet numbers which are typical for a process such as gravitational settling, used commonly in industry. For low particle volume fraction ($\varepsilon < 0.003$), the effect on the micro-convection was negligible. For high particle volume fractions ($0.1 \leqslant \varepsilon \leqslant 0.3$) the enhancement can be significant and can be 100% higher than pure heat conduction.

A close scrutiny of the results revealed that by introducing a modified form of Péclet number $(Pe' = Pe \times \varepsilon^{3/4})$, which combines particle volume fraction and the cell Péclet number, enhanced heat transfer could be expressed as a polynomial function of Pe'. The usefulness of such a correlation was demonstrated in the case of a suspension showing distributed particle fall velocities by computing expected errors in the estimated enhanced heat transfer based only on the mean particle fall velocity.

REFERENCES

1. A. Bejan, *Convection Heat Transfer*. Wiley, New York (1984).
2. S. L. Soo, Heat transfer due to convective interaction in fluid-solid mixtures, *ASME*, 90-*WA/HT*-14, Nov. 25–30 (1990).
3. L. G. Leal, On the effective conductivity of a dilute suspension of spherical drops in the limit of low particle Péclet number, *Chem. Eng. Commun.* **1**, 21–31 (1973).
4. C. W. Sohn and M. M. Chen, Microconvective thermal conductivity in disperse two-phase mixtures as observed in a low velocity Couette flow experiment, *J. Heat Transfer*, **103**, 47–51 (1981).

5. S. K. Gupte, S. G. Advani and P. Huq, A cell model to investigate the influence of fall velocity distribution on transport processes in a sedimenting suspension, February 1993. Presented at the 64th Annual Society of Rheology Meeting, Santa Barbara, California.
6. G. K. Batchelor, *An Introduction to Fluid Dynamics*, Cambridge University Press, Cambridge (1967).
7. J. Happel and H. Brenner, *Low Reynolds Number Hydro-*

dynamics, pp. 130–133. Kluwer, Dordrecht (1991).
8. J. Happel, Viscous flow in multiparticle systems: slow motion of fluids relative to beds of spherical particles. *AIChE J.* **4**, 197–201 (1958).
9. R. B. Bird, R. C. Armstrong and O. Hassager, *Dynamics of Polymeric Liquids*, Vol. 1. Wiley, New York (1987).
10. C. A. J. Fletcher, *Computational Techniques for Fluid Dynamics*, Vol. I. Springer, New York (1991).